The Journal of Experimental Biology 208, 2191-2203
Published by The Company of Biologists 2005
doi:10.1242/jeb.01616

The *C. elegans* T-type calcium channel CCA-1 boosts neuromuscular transmission

Katherine A. Steger[1,*], Boris B. Shtonda[1,*], Colin Thacker[2], Terrance P. Snutch[2] and Leon Avery[1,†]

[1]*Department of Molecular Biology, University of Texas, Southwestern Medical Center, Dallas, TX 75390, USA* and
[2]*Biotechnology Laboratory, University of British Columbia, Vancouver, BC, Canada*

*These authors contributed equally to this work
†Author for correspondence (e-mail: leon@eatworms.swmed.edu)

Accepted 19 February 2005

Summary

Low threshold-activated or T-type calcium channels are postulated to mediate a variety of bursting and rhythmic electrical firing events. However, T-type channels' exact physiological contributions have been difficult to assess because of their incompletely defined pharmacology and the difficulty in isolating T-type currents from more robust high threshold calcium currents. A current in *C. elegans* pharyngeal muscle displays the kinetic features of a T-type calcium channel and is absent in animals homozygous for mutations at the *cca-1* locus (see accompanying paper). *cca-1* is expressed in pharyngeal muscle and encodes a protein (CCA-1) with strong homology to the α_1 subunits of vertebrate T-type channels. We show that CCA-1 plays a critical role at the pharyngeal neuromuscular junction, permitting the efficient initiation of action potentials in response to stimulation by the MC motor neuron. Loss of *cca-1* function decreases the chance that excitatory input from MC will successfully trigger an action potential, and reduces the ability of an animal to take in food. Intracellular voltage recordings demonstrate that when wild-type *cca-1* is absent, the depolarizing phase of the pharyngeal action potential tends to plateau or stall near –30 mV, the voltage at which the CCA-1 channel is likely to be activated. We conclude that the CCA-1 T-type calcium channel boosts the excitatory effect of synaptic input, allowing for reliable and rapid depolarization and contraction of the pharyngeal muscle. We also show that the pharyngeal muscle employs alternative strategies for initiating action potentials in certain cases of compromised MC motor neuron function.

Supplementary material available online at
http://jeb.biologists.org/cgi/content/full/208/12/2191/DC1

Key words: calcium channel, T-type channel, neuromuscular junction, *Caenorhabditis elegans*, action potential.

Introduction

Low voltage-activated (LVA) or T-type calcium currents were first described in vertebrate cells in the mid 1980s (Armstrong and Matteson, 1985; Carbone and Lux, 1984; Nilius et al., 1985). In addition to being activated by small depolarizations from resting potential, T-type currents are 'tiny', with a unitary conductance of ~5–8 pS, and 'transient', exhibiting fast inactivation (for a review, see Perez-Reyes, 2003). T-type currents also deactivate slowly, resulting in substantial tail currents after depolarizing pulses. Finally, T-type currents display a strong voltage dependence of inactivation, and can effectively be deinactivated by hyperpolarizing pulses (Bean and McDonough, 1998). In mammals, different types of T-type calcium channel are encoded by three distinct α_1 subunit genes (α_{1G}/Cav3.1, α_{1H}/Cav3.2 and α_{1I}/Cav3.3) (Cribbs et al., 1998; Lee et al., 1999; McRory et al., 2001; Monteil et al., 2000a,b; Perez-Reyes et al., 1998).

While T-type calcium currents have been observed in a wide variety of cell types and tissues, their physiological relevance is not completely understood. Studies have implicated T-type conductances in the pacemaker current of the cardiac sino-atrial node (Hagiwara et al., 1988), contraction of vascular smooth muscle (Hansen et al., 2001), secretion of aldosterone from the adrenal glomerulosa (Cohen et al., 1988), bursting and rhythmic firing behavior in a variety of central neurons (reviewed by Huguenard, 1996), the amplification of excitatory post-synaptic potentials (EPSPs) in pyramidal neurons (Gillessen and Alzheimer, 1997; Urban et al., 1998) and neurotransmitter release from retinal bipolar cells (Pan et al., 2001). None of these functions has been directly linked to the loss of function of a particular α_1 subunit-encoding gene. Rather, the physiological roles of T-type channels are largely inferred from electrophysiological characterization and from the effects of a limited set of pharmacological blocking agents. The lack of specificity of these blocking agents, as well as the difficulty of isolating T-type calcium currents from more-

robust high voltage activated currents makes the inference of function difficult. In one instance, the α_{1G} (Cav3.1) subunit has been knocked out in a mouse model, generating a specific defect in thalamocortical relay neurons (Kim et al., 2001). However, the physiological functions of specific T-type channels in many tissues remain uncertain.

When reporting the cloning of the α_{1G} T-type channel subunit, the authors noted that the GenBank entry with the highest homology to α_{1G} was C54D2.5, a predicted protein from the genome of the free-living nematode *C. elegans* (Perez-Reyes et al., 1998). In the present study, we characterize the gene *cca-1* encoding that predicted protein, and its role in the feeding behavior of the worm.

C. elegans subsists on bacteria encountered in the soil, and feeds by rhythmically contracting and relaxing a neuromuscular pharynx, thus sucking food in. The pharynx consists of three regions: the corpus is closest to the mouth of the worm, the terminal bulb connects to the intestine, and the two are linked by a slender isthmus (Albertson and Thomson, 1976). Contraction and relaxation of the corpus and anterior isthmus muscles pulls in and traps bacteria (Avery, 1993b; Seymour et al., 1983). Contractions of the terminal bulb, which occur in synchrony with corpus contractions (Avery, 1993a), grind up the bacteria and push the food through a valve into the intestine (Doncaster, 1962). The near-simultaneous contraction of the corpus, anterior isthmus and terminal bulb is referred to as a 'pump'. Bacteria are transported from the corpus to the terminal bulb by a second motion, called an isthmus peristalsis (Avery and Horvitz, 1987).

The *C. elegans* pharynx contains a small nervous system that seems to play a modulatory role in the control of pharyngeal activity. Pumping continues when all the pharyngeal neurons are ablated with a laser (Avery and Horvitz, 1989), but the cholinergic motor neuron MC is necessary for the rapid pumping normally exhibited by worms and seems to act as a pacemaker. Worms lacking MC function are viable, but pump at a much-reduced rate (Avery and Horvitz, 1989; Raizen et al., 1995). Thus, the pharyngeal muscle is capable of rhythmic depolarization and contraction in the absence of pharyngeal neuronal activity, although the nervous system plays an important role in modulating the rate of pharyngeal pumping.

We have found that the *cca-1*gene product is intimately involved in the process of depolarization and action potential initiation in the *C. elegans* pharynx. In the accompanying paper, Shtonda and Avery describe a current in pharyngeal muscle that displays T-type kinetics (Shtonda and Avery, 2005). Wild-type *cca-1* is necessary for the expression of this current, suggesting that *cca-1* encodes a T-type α_1 subunit that functions in the pharyngeal muscle. Cloning and characterization of *cca-1* gene products confirms a strong similarity to vertebrate T-type channels, but analysis of *cca-1* mutants through electrophysiological techniques reveals a previously undescribed role for T-type calcium channels at the neuromuscular junction, where they aid in triggering action potentials in response to stimulation by motor neurons. Because the function of CCA-1 resembles those inferred from pharmacological blockade of T-type currents in vertebrates, yet can be traced to the loss of function of a single gene product, our description of CCA-1 provides significant insight into the roles of vertebrate T-type channels.

Materials and methods

General methods and strains

Caenorhabditis elegans (Maupas, 1900) were cultured and handled as described previously (Sulston and Hodgkin, 1988) with the following modifications: worms were routinely grown on NGMSR plates (Avery, 1993a) without nystatin. All worms were maintained at 20°C on *E. coli* strain HB101 (Boyer and Roulland-Dussoix, 1969). The wild-type strain was *C. elegans* variety Bristol, strain N2. Mutant strains were JD21 *cca-1(ad1650) X*, TS22 *cca-1(gk30) X*, DA465 *eat-2(ad465) II*, JD313 *eat-2(ad465) II*; *cca-1(ad1650) X*, CB245 *unc-17(e245) IV*, JD315 *unc-17(e245) IV*; *cca-1(ad1650) X*, RM1613 *snt-1(md290) II*, JD318 *snt-1(md290) II*; *cca-1(ad1650) X*, TS33 *vaIs3(pcca-1::GFP)* and TS321 *vaIs24(cca-1::GFP).*

cDNA cloning

C. elegans poly(A)$^+$ RNA was converted to cDNA using the RNase H$^-$ MMLV reverse transcriptase, SuperScript II (Invitrogen, Carlsbad, CA, USA) and the primer T22V (oligo(dT)$_{22}$V, where V=A, G or C), following the method of Regan et al. (2000). Then, PCR was performed using an SL1-specific primer containing a *Not*I restriction site (5′-ATAA-GAATGCGGCGCGGTTTAATTACCCAAGTTTG-3′) in combination with the antisense primer cca-30 (5′-GGGGGTACCGTAGAGGAAACATGGACCGGA-3′), which anneals within the *cca-1* 3′ UTR and introduces a *Kpn*I restriction site. The resulting PCR products were digested with *Not*I–*Kpn*I, and cloned into pBluescript SKII. Because full-length clones were difficult to propagate in *E. coli*, RT-PCR products were also digested with appropriate restriction enzymes to clone overlapping cDNA fragments. The use of this procedure prevented us from making an exact assessment of the relative frequency of different *cca-1* splice variants. Clones were isolated and sequenced on both strands. In some cases the RT-PCR products were sequenced directly.

Sequence alignments

Sequences were aligned using the ClustalW program, and the shaded alignment was generated with GeneDoc (Pittsburgh Supercomputing Center; http://www.psc.edu/biomed/genedoc). The phylogenetic tree in Fig. S2 in supplementary material was constructed by aligning the sequences with the ClustalX program and plotting the alignments using TreeView.

Analysis of cca-1 *expression*

Two different *cca-1*::GFP fusion constructs were used to examine the expression pattern of the calcium channel gene. The first construct fused an 8074 base pair (bp) fragment of the

cca-1 gene comprising 5.4 kb of sequence upstream of the putative *cca-1* initiation codon and three coding exons to GFP. The *cca-1* fragment was amplified by PCR using the primers cca-11 (5′-TGATGATAGGACGCTGGTCA-3′) and cca-12 (5′-TGTTCCGACAGCTGCAGAGT-3′). The PCR product was digested with *Pvu*II and *Pst*I and cloned into pBluescript SK. The GFP gene and *unc-54* 3′ UTR regions of pPD95.69 (a gift from A. Fire, Carnegie Institution of Washington, USA) were isolated by digestion with *Pst*I and *Eag*I and the resulting 1.9 kb fragment was inserted into pBluescript, 3′ to the *cca-1* sequences, to generate an in-frame *cca-1*::GFP fusion (pcca-1::GFP). Transgenic worms were generated by injecting 20 ng/μl of pcca-1::GFP with 50 ng/μl of plin-15(+) and 50 ng/μl of pBluescript SK into *lin-15(n765ts)* X worms. Transformants were isolated by rescue of the Lin-15 multivulval phenotype.

The second *cca-1::GFP* construct was generated using a PCR based fusion approach similar to that described by (Hobert, 2002). A total of three PCR products were used. The first two products (overlapping fragments encompassing the entire *cca-1* genomic locus) were amplified using wild-type DNA as template (Fig. 1A). The first product (10676 bp) was generated using the sense primer cca-35 (5′-GAGTC-TAGATGAGACGCACA-3′), which annealed approximately 5.8 kb upstream of the first exon, and antisense primer cca-40 (5′-GCAAGTGTGTAACCCGTTG-3′), located in exon nine. The second product extended from intron six up to the predicted stop codon and was amplified using the sense primer cca-38 (5′-TTGCTCGTTCAACACCACTC-3′), and antisense oligo cca-34 (5′-CTTTGGCCAATCCCGGGGATCTAAAG-CAGACTTGTGTGATCCA-3′). Next, GFP sequences from the plasmid pPD95.75 (a gift from A. Fire, Carnegie Institution of Washington, USA) were amplified using the sense primer cca-39 (5′-TGGATCACACAAGTCTGCTTTAGATCCCC-GGGATTGGCCAAAG-3′) and oligo GFP3′ UTR (5′-TTC-ACCGTCATCACCGAAAC-3′). Equimolar amounts of the 3′ *cca-1* and GFP PCR products were then fused by PCR resulting in an in-frame carboxyl-terminal translational fusion. The sequences of the internal oligos used for the PCR fusion were cca-36 (5′-CATCCGCGTATTTCACGTTG-3′) and GFP3′ (5′-ATCCGCTTACAGACAAGCTG-3′). Transgenics were generated by injecting 20 ng/μl of the 10676 bp 5′ *cca-1* PCR product with 20 ng/μl of the 3′ *cca-1::GFP* fusion product, and 60 ng/μl of pBluescript SK into *cca-1(ad1650) X* worms. GFP expression is contingent on recombination of the 5′ *cca-1* PCR product with the overlapping 3′ *cca-1*::GFP fusion. After transformed lines carrying each of the constructs were established, the extrachromosomal arrays were integrated using γ-irradiation. The resulting strains were backcrossed to wild-type worms, generating strain TS33 carrying the pcca-1::GFP construct and TS321 carrying the full-length PCR-fusion based construct.

Chemicals

Chemicals used were the creatinine sulfate complex of serotonin (5-hydroxytryptamine; Sigma, Aldrich, St Louis, MO, USA; cat. no. H-7752) and the hydrogen tartrate salt of nicotine (Sigma; cat. no. N-5260).

Measurement of pumping rate

Motions of the terminal bulb grinder plates were used to count pumps. Twenty gravid adult worms of approximately the same size and age were placed on a lawn of *E. coli* HB101 and allowed to acclimate for at least 1 h. Counts were made at room temperature (approximately 23°C). Each worm was observed for 30 s and each recorded number of pumps was doubled to generate a ‘pumps per minute’ value. Therefore, N=20 for each calculation of pumping rate. We note, however, that each experiment was performed at least three separate times, and data shown are representative. To determine the statistical significance of a difference in pumping rate between two strains, we used the two-tailed heteroscedastic t-test.

Extracellular recordings and statistical analysis

Extracellular recordings (electropharyngeograms) were recorded on dissected pharynxes as previously described (Avery et al., 1995). For all recordings, the bath included 1 μmol l^{-1} serotonin. Recordings were made with a Patch PC-501A amplifier (Warner Instruments, Hamden, CT, USA), a Digidata 1322A acquisition system (Axon Instruments Inc, Union City CA, USA) and Axoscope 8.1 software (Axon Instruments). All recordings were filtered with a low-pass 5 Hz filter and a high-pass 20 Hz filter. Traces shown in figures underwent an additional low-pass filter of 350 Hz using Clampfit 8.1 software (Axon Instruments). The sampling rate was 10 KHz.

The heights of E1 and E2 peaks, the time intervals between them and the log of the ratio of the E1 and E2 heights were recorded for each of the first 12 action potentials from five *cca-1* mutant worms and eight wild-type worms. The data were analyzed by two-level nested ANOVA, followed by an F-test of the ratio of the mean square between genotypes to the mean square within genotypes.

The ratio of I-phase spikes to action potentials was calculated by direct counting of spikes in a 1 min recording for each of six to eight worms of each genotype. Any sharp, brief depolarizing spike that was not immediately followed by an action potential was assumed to be an I-phase spike. In *snt-1*, *snt-1; cca-1* and *unc-17; cca-1* worms, action potentials are sometimes preceded by a series of depolarizations, the last of which triggers an action potential. All but the last of the series were counted as I-phase spikes. Because the occurrence of I-phase spikes is more common in some individual worms than others, we have summed the data from all the worms of each genotype.

Intracellular voltage recordings

Intracellular voltage recordings were performed using the Axoclamp 2B with the HS-2A 0.1LU headstage as described by Davis et al. (1999), with the following exceptions. The recording chambers and extracellular solution were the same as used by Shtonda and Avery (2005), and pipette solution was

3 mmol l^{-1} potassium acetate, 10 mmol l^{-1} KCl. Micropipettes were pulled from 1/0.58 mm borosilicate capillaries (A-M Systems, Carlsborg, WA, USA) on the P-2000 puller; they had resistance of 50–100 MΩ when filled with the pipette solution. Data were acquired using custom-designed Labview software (Raizen and Avery, 1994) at a sampling rate of 2 KHz. Another Labview program was used to algorithmically extract, align, differentiate and average action potentials from recorded voltage traces

For analysis, regions of recorded traces were chosen in which the resting membrane potential had completely stabilized (normally 2–3 min after electrode insertion). The micropipette tip potential was measured after electrode removal and subtracted from the trace in order to compensate for the small drift of the tip potential that usually occurred during penetration into the cell. The average tip potential change was 4.3±5.8 mV in the positive or negative direction (N=48, mean ± S.D.). Action potentials were recognized when the following conditions were met in this order: (1) the analyzed point in the trace was within the specified baseline (between –90 and –50 mV for the wild type, adjusted for mutants with higher resting potential); (2) the analyzed point was followed within 200 ms by at least one point at voltage higher by 50 mV or more, and (3) the average rate of voltage change in the 50 ms following the analyzed point exceeded 0.5 V s^{-1}. The end of the action potential was determined as the first point within the baseline where the voltage slope over the next 25 ms was positive. To align action potentials, we minimized the sum of squared differences between the rising phase segment from –20 to 10 mV (this segment was chosen because it was the least variable) and a vertical line at 0 ms.

The resting membrane potential was extracted as all points in the analyzed region of the trace within the baseline for which the average rate of change of voltage over the next 100 ms was between –0.02 and +0.02 V s^{-1}. These points were averaged over a 1–3 min interval to calculate the resting membrane potential for a given pharynx.

Results

cca-1 *encodes a protein similar to vertebrate T-type calcium channel* α_1 *subunits*

The *C. elegans* C54D2.5 open reading frame was originally used to predict the existence of T-type channels in vertebrates (McRory et al., 2001; Perez-Reyes et al., 1998). To determine the actual amino acid sequence of predicted peptide C54D2.5, we isolated overlapping cDNA clones from *C. elegans* mRNA. We found that the C54D2.5 transcript differs significantly from the GeneFinder prediction and that several transcripts are generated as a result of alternative splicing (shown in Fig. 1A,B). Our analysis revealed that C54D2.5 consists of at least 30 exons encompassing a region of approximately 14 kilobases (kb; Fig. 1A). Four alternatively spliced transcripts were identified and each encodes a predicted gene product that displays membrane topology consistent with a voltage-gated calcium channel α_1 subunit. All predicted gene products possess four domains (I–IV) each consisting of six membrane-spanning segments and a pore loop (Fig. 1B). Each set of S1–S6 membrane-spanning domains regions includes an S4 voltage sensor segment containing repeated basic residues. Because of these characteristic structural features, we named the gene *cca-1* for calcium channel alpha 1-like subunit.

All of the full-length cDNAs we isolated were *trans*-spliced

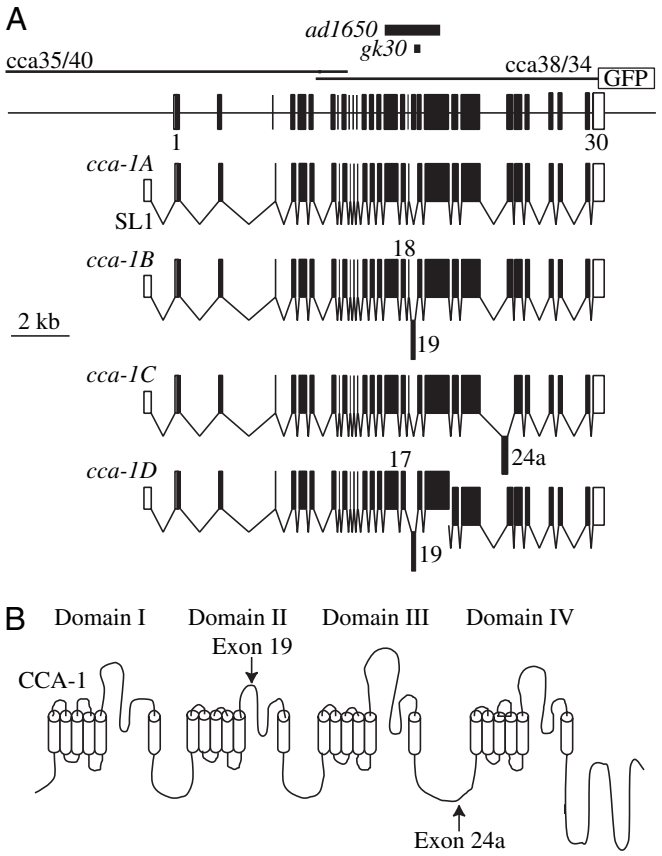

Fig. 1. Structure of the *cca-1* gene and CCA-1 calcium channel. (A) Intron–exon structure of *cca-1*. Coding exons are represented by filled rectangles, non-coding exons by open rectangles. The *ad1650* and *gk30* deletions are indicated by bars. All cDNAs characterized were found to be *trans*-spliced at the 5′ end to the SL1 leader RNA (SL1). The most-abundant transcript, *cca-1A*, is composed of all exons except exon 19. Splice variant *cca-1B* uses an alternative splice donor in exon 18, which is spliced to exon 19. The *cca-1D* transcript splices exon 17 directly to exon 19. The inclusion of exon 19 would add amino acid residues to the pore loop region of domain II, and may have significant effects on the activity of the channel. Splice variant *cca-1C* uses an alternative 5′ splice donor for exon 24, which is predicted to result in the incorporation of an additional 15 amino acids in the III–IV loop. Sequences of the four splice variants have been submitted to GenBank under accession numbers AY313898 (*cca-1A*), AY313899 (*cca-1B*), AY313900 (*cca-1C*) and AY322480 (*cca-1D*). The PCR products used to generate the *cca-1*::GFP fusion constructs are diagrammed and labeled with the names of the primers used for amplification (cca35/40 and cca38/34). (B) Domain structure of CCA-1. Open cylinders indicate transmembrane domains, and the positions of the alternative exons found in splice variants B, C and D are shown.

to the 22 nucleotide base pair (bp) SL1 leader RNA found on the 5′ ends of many *C. elegans* mRNAs (Blumenthal and Steward, 1997) and were similar in structure except for variations involving alternative splicing of exons 18, 19 and 24. The most commonly isolated transcript, *cca-1A* (6129 base pairs in length) was composed of all exons except exon 19 (Fig. 1A), and encodes a predicted product of 1837 amino acids. The *cca-1B* transcript uses an alternative splice donor site within exon 18, which is spliced to exon 19 resulting in a 6273 bp transcript encoding an 1885 amino acid product. The *cca-1D* transcript differs in that exon 17 is spliced directly to exon 19 generating a transcript of 6150 bp and a predicted 1844 amino acid polypeptide. The alternative splicing found in the A, B and D variants is predicted to generate α_1 subunits that only differ in the IIS5-IIS6 loop, which includes the P-loop region for domain II. Finally, we have found that the *cca-1C* transcript is identical in exon composition to the *cca-1A* variant except for the use of an alternative splice acceptor for exon 24 (exon 24a in Fig. 1A), which results in the incorporation of an additional 15 amino acids in the III-IV loop of the encoded gene product.

The membrane spanning regions of the most abundant *cca-1* splice variant (CCA-1A) show significant sequence conservation with the corresponding regions of the vertebrate subunits α_{1G}– α_{1H} and α_{1I}. CCA-1 resembles the vertebrate T-type α_1 subunits in containing aspartate residues in the P-loops of the third and fourth domains (alignment presented in Fig. S1 in supplementary material). Calcium channel α_1 subunits that contribute to high voltage-activated (HVA) channels contain glutamate residues at these positions (Perez-Reyes, 2003). Furthermore, in contrast to HVA calcium channels, the domain I-II linker of the CCA-1 protein lacks a β subunit-binding site, and the carboxyl region lacks both an E-F hand region and a calmodulin-binding domain (data not shown). Construction of a phylogenetic tree including all the putative calcium channel α_1 subunits from human, *Drosophila melanogaster* and *C. elegans* demonstrates that CCA-1 is more closely related to vertebrate T-type α_1 subunits than to other α_1 subunits (Fig. S2 in supplementary material). CCA-1 is most similar to vertebrate α_{1I} (42% identity), and is also closely related to α_{1G} (39% identity) and α_{1H} (37% identity). These similarities suggest that CCA-1 is likely to function as a T-type calcium channel α_1 subunit.

In order to determine the physiological roles of CCA-1, we examined two *cca-1* deletion alleles that are likely to severely compromise *cca-1* function. *ad1650*, which we isolated from a deletion library by PCR screening, is a 2.5 kb deletion that removes exons encoding half of the second and most of the third repeated domains, and also causes a frameshift (Fig. 1A; see S1 in supplementary material). *gk30*, a gift from the *C. elegans* Reverse Genetics Core Facility (University of British Columbia, Canada), contains a smaller deletion that removes a portion of the P-loop of domain II along with alternatively spliced exon 19, causes a frameshift and results in a prematurely truncated protein (Fig. 1A; see S1 in supplementary material). The *gk30* allele also contains a complex rearrangement outside the *cca-1* coding region. Shtonda and Avery (2005) recently demonstrated that *cca-1(ad1650)* mutants lack the T-type current observed in wild-type pharyngeal muscle, providing further evidence that *cca-1* encodes the *C. elegans* T-type calcium channel.

A cca-1 *reporter construct is expressed primarily in neurons and muscles*

We determined the expression pattern of *cca-1* by constructing two different *cca-1*::GFP fusions. The larger construct, created by PCR and *in vivo* recombination, carries GFP fused in-frame at the predicted *cca-1* carboxyl terminus (Fig. 1A; see Materials and methods for a full description of the construct). Transgenic animals carrying this construct show GFP fluorescence in a variety of cells, with robust expression in the pharyngeal muscle (Fig. 2). We also observed GFP expression in many neurons, including specific subsets in the head, pharynx, ventral nerve cord and anal ganglia. A smaller construct with fewer intron sequences (pcca-1::GFP) is localized differently within cells and reveals GFP fluorescence in body wall muscle, distal tip cells, enteric muscle and cells of the posterior intestine (Fig. S3 in supplementary material). Within the pharynx, *cca-1* expression is observed in most if not all pharyngeal muscle cells

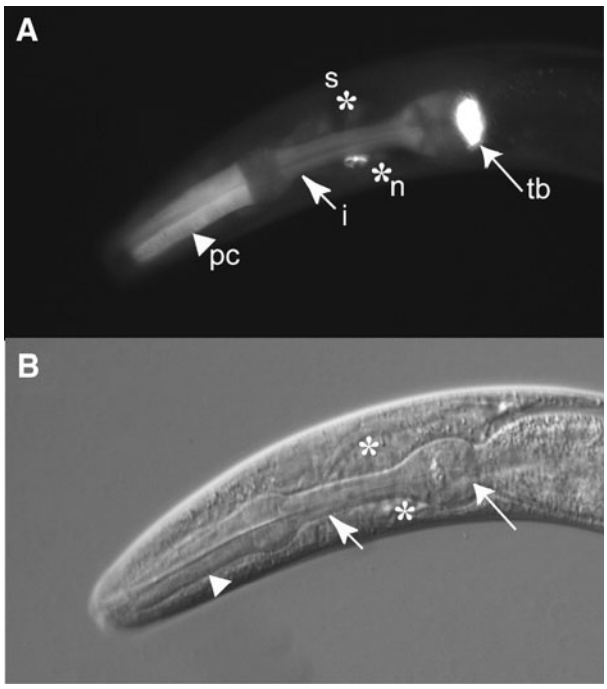

Fig. 2. A *cca-1::GFP* gene fusion is expressed in the pharyngeal muscle. (A) Transgenic animals carrying an extra-chromosomal array including a full-length *cca-1::GFP* fusion (strain TS321) exhibit GFP fluorescence in all pharyngeal muscle including cells of the procorpus (pc), metacorpus, the isthmus (i) and in the terminal bulb (tb). The intense staining in the posterior of the terminal bulb is localized to the pm8 muscle cell. The asterisk indicates expression in extrapharyngeal neurons (n) and sheath cells (s) in the head. A differential interference contrast (DIC) image of the same worm is shown in B for comparison. Labeling as in A.

but is most prominent in those of the procorpus (labeled 'pc' in Fig. 2) and in pm8, the most posterior cell in the terminal bulb (labeled 'tb' in Fig. 2). Expression of *cca-1* in pharyngeal muscle cells is consistent with the observation of Shtonda and Avery (2005) of a T-type current in the *C. elegans* pharynx, which is absent in *cca-1(ad1650)* mutants.

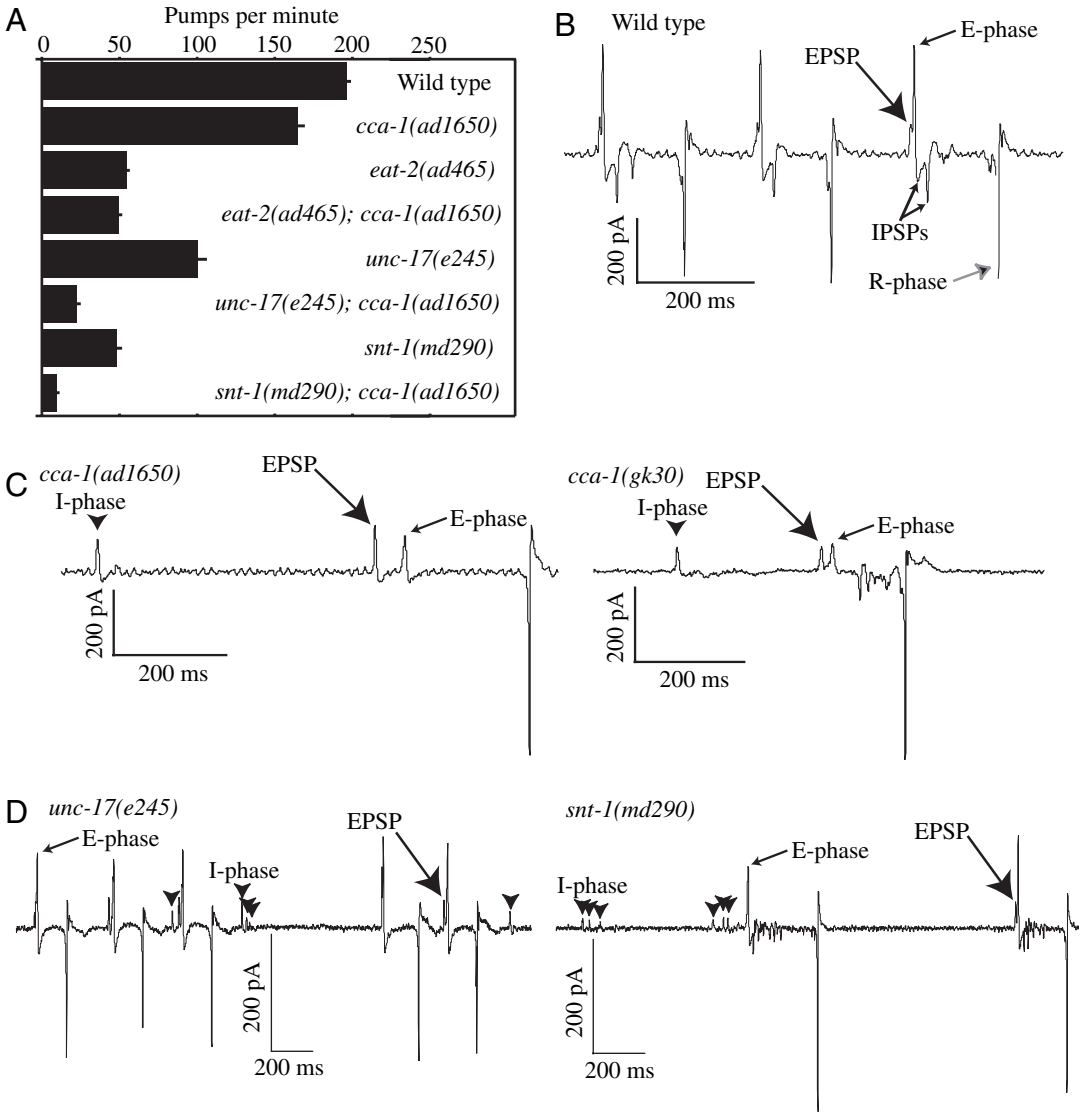

Fig. 3. Loss of *cca-1* function or reduction of MC neurotransmission compromises action potential initiation and reduces pharyngeal pumping rates. (A) Effect of *cca-1* mutations on the pumping rates of intact worms in the presence of *E. coli* HB101. Results are shown as the mean number of pumps per minute. Values are means ± standard error of the mean (S.E.M.). *N*=20 worms for each data point. See Materials and methods for additional details. (B) In electropharyngeograms (EPGs) from wild-type worms, a small EPSP (excitatory post-synaptic potential) precedes each excitation (E-phase) spike. An EPSP is marked with a large black arrow while an E-spike is marked with a small black arrow. The action potential terminates with a large negative repolarization (R-phase) spike (large gray arrow). Smaller negative spikes between E and R represent inhibitory post-synaptic potentials (IPSPs) from the inhibitory motor neuron M3 (Dent et al., 1997; Raizen and Avery, 1994). (C) In EPGs from *cca-1* mutants homozygous for either of two loss-of-function alleles (*ad1650* or *gk30*), small, delayed E-phase spikes (small arrows) follow the EPSPs. EPGs from *cca-1* mutants also contain interpump phase (I-phase) spikes between pumps (arrowheads). (D) Effect on EPG traces of defects in MC neurotransmission. *unc-17* encodes a membrane transporter that loads acetylcholine into synaptic vesicles within the cholinergic neurons, including the MC motor neuron. *e245* is a viable missense allele of *unc-17* (Alfonso et al., 1993). Null mutations of *unc-17* are lethal. EPGs from *unc-17(e245)* mutants contain occasional I-phase spikes (arrowheads), because the low acetylcholine content of synaptic vesicles reduces the success rate of MC neurotransmission. *snt-1* encodes synaptotagmin, a vesicle-associated protein necessary for effective calcium-stimulated release of neurotransmitter. *snt-1(md290)* is a putative null allele of synaptotagmin (Nonet et al., 1993). EPGs from *snt-1(md290)* mutant worms contain many I-phase spikes (arrowheads), often occurring in clusters, as a result of uncoordinated neurotransmitter release. Because EPGs recorded from different individual worms show some variation, we have annotated the features that consistently differ between worms of different genotypes. Unmarked differences are likely to be due to individual variation.

Table 1. *Effect of* cca-1 *on electrical activity in the pharynx*

Genotype	I-spikes/ 100 APs	No. animals	No. APs	E/EPSP height	EPSP to E time (ms)
Wild type	2.6	8	1450	3.4±0.3	6.7±0.3
cca-1(ad1650)	14.4	7	640	1.3±0.1*	26.7±2.3*
unc-17(e245)	9.5	6	803	2.3±0.1	12.2±0.7
unc-17(e245); cca-1(ad1650	288.3	6	123	N/D	N/D
snt-1(md290)	118.7	6	134	N/D	N/D
snt-1(md290); cca-1(ad1650)	717.8	6	45	N/D	N/D

I-phase activity observed on EPG traces is expressed as the number of I-phase spikes per 100 action potentials (AP). For the calculation of the I-phase/AP ratio, individual animals were observed for 1 min each, and every AP was assessed and counted. The number of animals analyzed and the total number of action potentials (APs) observed are shown for each genotype. See Materials and methods for additional details.

The E/EPSP height column shows the average ratio between the height of the E-phase spike and the height of the EPSP spike (mean ± S.E.M.). The average interval between the peaks of the E-phase and EPSP spikes is shown in ms (mean ± S.E.M.).

N/D, not determined.

*Significantly different from wild type, $P<0.01$.

Loss of cca-1 *function disrupts pharyngeal pumping*

Because *cca-1* expression is observed in the pharynx (Fig. 2) and the *ad1650* deletion mutation eliminates an inward current in the pharyngeal muscle (Shtonda and Avery, 2005), we investigated the effects of *cca-1* mutations on feeding behavior. First, we found that pharyngeal pumping in *cca-1(ad1650)* mutants is significantly slower than in wild-type worms (Fig. 3A; $P<0.005$ for this comparison). We then examined the electrical activity of wild-type and *cca-1* mutant worms using electropharyngeograms (EPGs; Raizen and Avery, 1994). The EPG records changes in the membrane potential of the pharyngeal muscle, and reflects the time derivative of the muscle action potential. The EPG of a normal action potential consists of a large positive E-phase spike, representing pharyngeal muscle excitation, a plateau phase where membrane potential is largely stable, and a large negative R spike, representing repolarization (Fig. 3B). E-phase spikes reflect calcium entry into the pharyngeal muscle through L-type voltage-gated calcium channels encoded by *egl-19* (Lee et al., 1997). In addition, the activity of the MC motor neuron is visible on an EPG trace. Preceding each E-phase spike is a small deflection or shoulder, representing an excitatory post-synaptic potential (EPSP; Raizen et al., 1995). This EPSP results from the activation of nicotinic receptors on the pharyngeal muscle surface by acetylcholine from MC (McKay et al., 2003; Raizen et al., 1995).

EPGs reveal that the depolarization of the pharyngeal muscle is abnormal in *cca-1* mutants. While EPGs from wild-type worms display a small EPSP before each large E-phase spike, *cca-1(ad1650)* and *cca-1(gk30)* deletion mutants often display two peaks of almost equal size in the excitation phase (Fig. 3C). *cca-1(ad1650)/cca-1(gk30)* heterozygotes have a similar phenotype, while heterozygotes carrying one wild-type and one mutant copy of *cca-1* are unaffected (data not shown). We suspect that the first spike in these M-shaped segments represents an EPSP, and the second spike is a small, delayed E-phase spike. Because the EPG trace represents the time derivative of the action potential, a small, late E-spike reflects a delay and a reduced slope in the rise in the pharyngeal muscle membrane potential in response to an EPSP. In wild-type pharynxes, E-phase spikes are, on average, 3.4 times the size of the EPSPs that precede them (Table 1). The average time interval between the peaks of the EPSP and E spikes is seven milliseconds (ms). In *cca-1(ad1650)* mutant worms, E-phase spikes average 1.3 times the size of their paired EPSPs and the time between peaks averages 27 ms (Table 1).

In addition to abnormalities related to E-phase spikes, EPGs from *cca-1(ad1650)* mutant worms contain more inter-pump phase (I-phase) spikes than wild-type EPGs (Fig. 3C, Table 1). I-phase spikes are small depolarizations occurring between action potentials and represent EPSPs that fail to trigger action potentials. They appear frequently in EPGs from worms with defects in synaptic transmission, and are not found in EPGs from worms whose MC neurons have been ablated (Raizen et al., 1995). For example, Fig. 3D shows EPGs recorded from two different mutant strains with defects in MC neurotransmission. *snt-1* encodes synaptotagmin (Nonet et al., 1993), a vesicle-associated protein necessary for effective calcium-stimulated release of neurotransmitter, while *unc-17* encodes a transporter that packs acetylcholine into synaptic vesicles (Alfonso et al., 1993). Both *snt-1(md290)* and *unc-17(e245)* mutants pump more slowly than wild-type worms (Fig. 3A), and their EPGs have many I-phase spikes (Fig. 3D and Table 1). The frequent I-phase spikes in *cca-1* mutants combined with the altered relationship of E-phase spikes to EPSPs suggest that *cca-1* mutants are defective in their ability to trigger pharyngeal muscle action potentials in response to MC stimulation. To further characterize the depolarization defect in *cca-1* mutant animals, we therefore employed intracellular voltage recordings of pharyngeal muscle activity.

Loss of cca-1 *alters the shape of the pharyngeal muscle action potential*

Recordings from wild-type pharynxes show a steeply rising

slope throughout the depolarization phase of the action potential. In contrast, recordings from *cca-1* mutant worms often contain exaggerated flattened regions or notches in the early phase of the muscle depolarization. Fig. 4A compares representative single traces from a wild-type worm and from a *cca-1(ad1650)* deletion mutant animal. Fig. 4C,D compares large numbers of action potentials from two worms of each genotype, and shows that pauses or dips in membrane potential are common in *cca-1(ad1650)* mutants, but rare in wild-type worms. (The traces shown are consistent with traces recorded

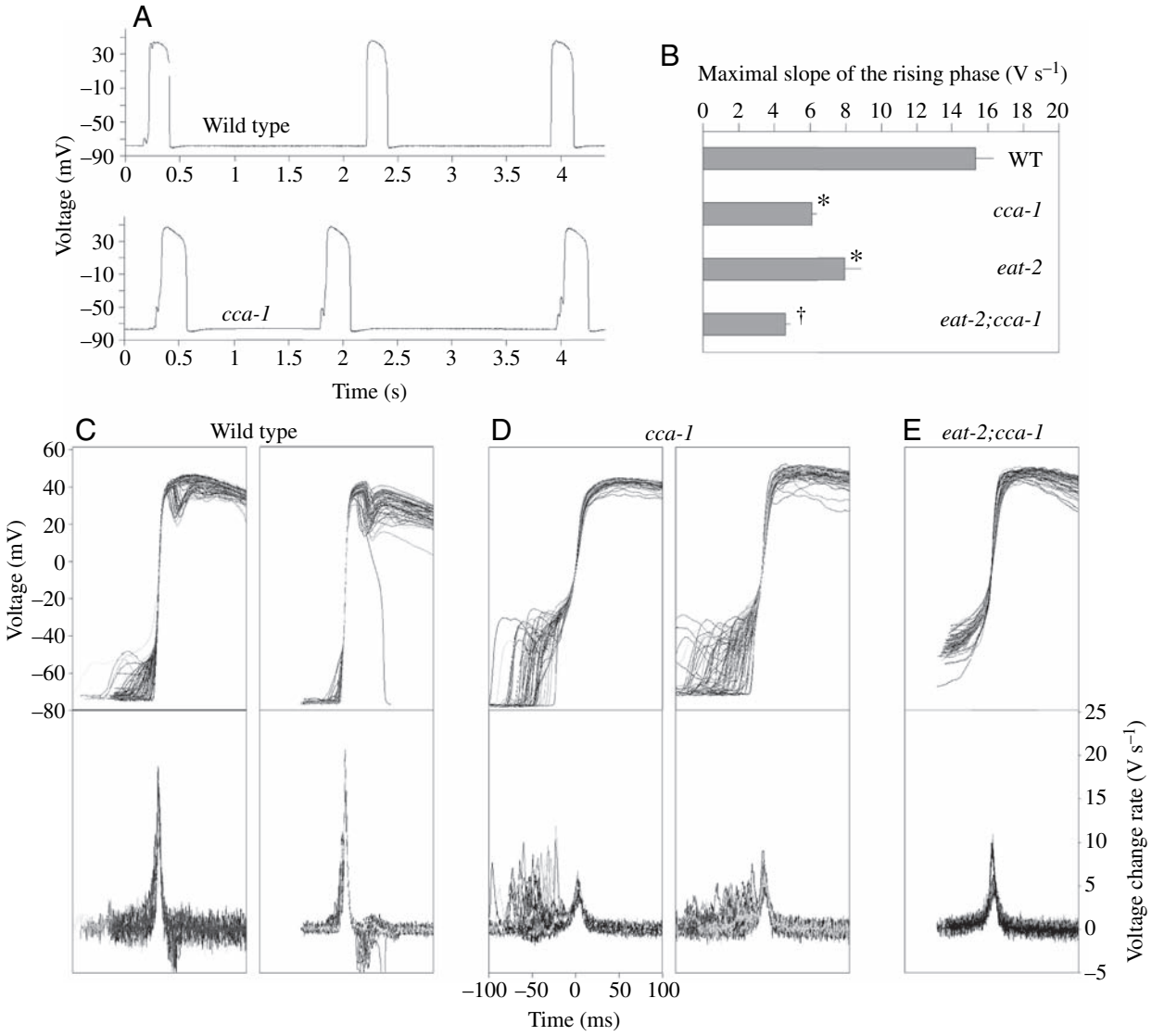

Fig. 4. Intracellular recordings reveal altered depolarization in action potentials from *cca-1* mutant pharynxes. (A) Sample intracellular voltage recordings from wild-type and *cca-1(ad1650)* mutant worms. While the depolarization phase of the wild-type action potential usually rises steeply and steadily from resting potential to a peak, action potentials from *cca-1* mutant worms often display a notch or flattened area early in depolarization. (B) Average maximal rising phase slopes for the wild-type, *cca-1*, *eat-2* and *eat-2*; *cca-1*. 50–100 differentiated and aligned action potentials were averaged for each individual pharynx. A peak slope for each individual pharynx was obtained from the averaged trace. This calculation was performed for 19 wild-type animals, 16 *cca-1* mutant animals, 14 *eat-2* mutant animals and 11 *eat-2; cca-1* double mutant animals. From the peak slopes for each individual, an average peak slope was calculated for each genotype, expressed as mean ± S.E.M. *Significantly different from the wild type; †significantly different from all other strains (P<0.005 for all comparisons, t-test). (C) (Top) Superimposed action potentials (with rising phases aligned) from two representative wild-type pharynxes. (Bottom) Time derivatives of the action potentials above. N=63 and 66 for left and right traces, respectively. (D) Same as in C for two representative *cca-1(ad1650)* worms; N=51 and 74 for left and right panels, respectively. While wild-type action potentials generally display a smooth steep rising phase, the majority of action potentials from *cca-1* mutant worms contain an initial depolarization, followed by a flattened area or notch. Plotting the time derivative of each action potential trace reproduces the EPG phenotypes of wild-type and *cca-1* mutant worms (compare with Fig. 3) with a small, delayed depolarization spike following each initial rise in membrane potential. (E) Action potentials from two representative *eat-2(ad465); cca-1(ad1650)* double mutants, labeled as in C and D. These action potentials lack the initial depolarization and plateau seen in *cca-1* single mutants, suggesting that early depolarization in a wild-type pharynx or *cca-1* mutant pharynx is mediated by the EAT-2-containing nicotinic receptor.

from a total of 19 wild-type and 16 *cca-1* mutant animals.) Membrane potential in *cca-1* mutants consistently stalls at around –30 mV, the potential at which the CCA-1 channel is expected to activate (Shtonda and Avery, 2005). If we calculate and plot the time derivatives of intracellular recordings from *cca-1* mutants, the plateau we observe in membrane potential becomes a valley between the initial MC-stimulated depolarization of the muscle membrane (the EPSP) and the fast upstroke of the action potential. Thus, plotting the time derivative of the intracellular voltage recording trace recreates the phenotype observed in *cca-1* mutant EPGs (Fig. 4C,D, lower panels). As a result of the notches and dips early in the rising phase of the action potential, the maximal speed of the action potential upstroke is decreased by about 2.5 times in *cca-1(ad1650)* mutants compared to wild-type worms (Fig. 4B). Thus, comparing the shapes of pharyngeal muscle action potentials in wild-type and *cca-1* mutant worms explains the abnormality we observed in the relationship of MC EPSPs to the pharyngeal muscle in *cca-1* mutants: the CCA-1 channel is necessary for a smooth, steep rise of membrane potential after an EPSP. CCA-1, a low-voltage activated channel, may serve as a bridge between the small membrane depolarization achieved by an EPSP and the EGL-19 L-type channel that activates at more-depolarized potentials.

Loss of cca-1 *enhances phenotypes caused by defects in synaptic transmission*

Because wild-type *cca-1* seems to be necessary for the efficient initiation of action potentials in response to MC EPSPs, we hypothesized that loss of *cca-1* function would increase the severity of phenotypes caused by abnormal synaptic release from MC. We therefore constructed double mutant strains of *cca-1(ad1650)* with mutations in *unc-17* or *snt-1*. As shown in Fig. 5 and Table 1, the combination of mutations in *cca-1* with mutations that decrease the effectiveness of MC neurotransmission severely compromises pharyngeal pumping. Both *unc-17; cca-1* and *snt-1; cca-1* mutant strains exhibit severely reduced pumping rates and high frequencies of I-phase spikes on EPGs. These data show that when synaptic release from MC is weakened, wild-type *cca-1* is crucial to the efficient generation of action potentials, and support a role for *cca-1* channels as a bridge between the MC EPSP and full membrane depolarization.

The C. elegans *pharynx adapts to loss of nicotinic MC signals by altering resting membrane potential, diminishing the role of CCA-1*

The MC motor neuron exerts its effects on the pharynx primarily through the activation of nicotinic receptors on the pharyngeal muscle surface. Acetylcholine from MC binds to nicotinic receptors, triggering cation influx and generating an EPSP. *eat-2* encodes a non-alpha nicotinic receptor subunit that is expressed in the pharyngeal muscle at the MC neuromuscular junction and participates in generation of EPSPs in response to MC signals (McKay et al., 2003). When *eat-2* function is eliminated, EPSPs are absent from EPG traces

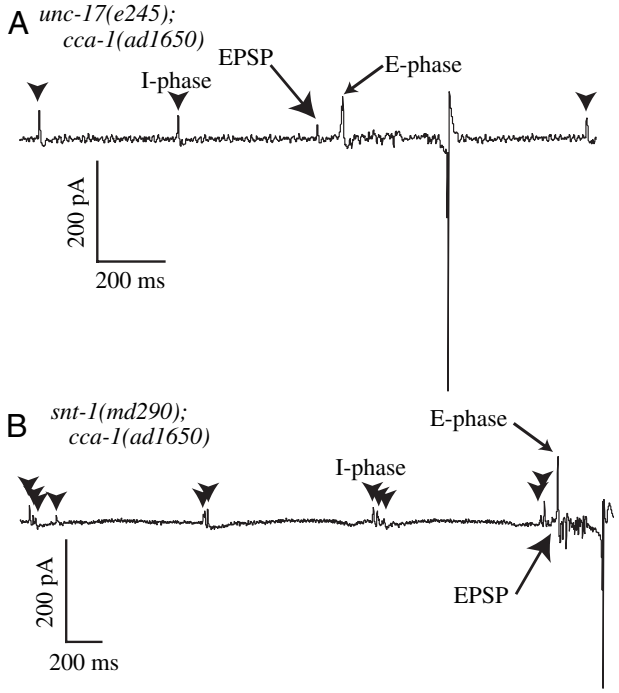

Fig. 5. CCA-1 activity is crucial for the efficient initiation of action potentials in animals with defects in cholinergic neurotransmission. (A) EPGs from *unc-17(e245); cca-1(ad1650)* double mutants contain many I-phase spikes, reflecting the fact that MC is often unsuccessful in triggering a pharyngeal muscle action potential. The frequency of I-phase spikes is far greater in an *unc-17(e245); cca-1(ad1650)* double mutant than in an *unc-17(e245)* single mutant (shown in Fig. 3D). (B) EPGs from *snt-1(md290); cca-1(ad1650)* mutant worms contain rare action potentials separated by many clusters of I-phase spikes. Again, the rate of failure of action potential generation is far greater in a *snt-1(md290); cca-1(ad1650)* double mutant than in a *snt-1(md290)* single mutant (shown in Fig. 3D). EPSPs are marked with large arrows. E-phase spikes are marked with small arrows. I-phase spikes are marked with arrowheads.

and mutant worms pump slowly (Fig. 3A, Fig. 4E and Fig. 6A). The same effects are seen in worms whose MC neurons have been ablated with a laser (Raizen et al., 1995). The mechanism by which *eat-2* mutants and other worms lacking MC function generate action potentials is poorly understood. The generation of action potentials in the absence of EAT-2 appears to be somewhat less efficient than in wild-type worms, as the maximal rate of rise of the action potential upstroke is reduced in *eat-2* mutants, as compared to wild-type worms (Fig. 4B). Since *cca-1* seems to be involved in improving the efficiency of action potential initiation by elevating pharyngeal muscle membrane potential to the threshold for EGL-19 opening, we suspected that *eat-2; cca-1* double mutant animals might have great difficulty generating action potentials, and be inviable. This hypothesis proved incorrect (see below), but led us to an understanding of how the *C. elegans* pharynx can adapt to deficits of MC function.

Double mutant animals carrying mutations in both *eat-2* and *cca-1* are almost indistinguishable from *eat-2* single mutants

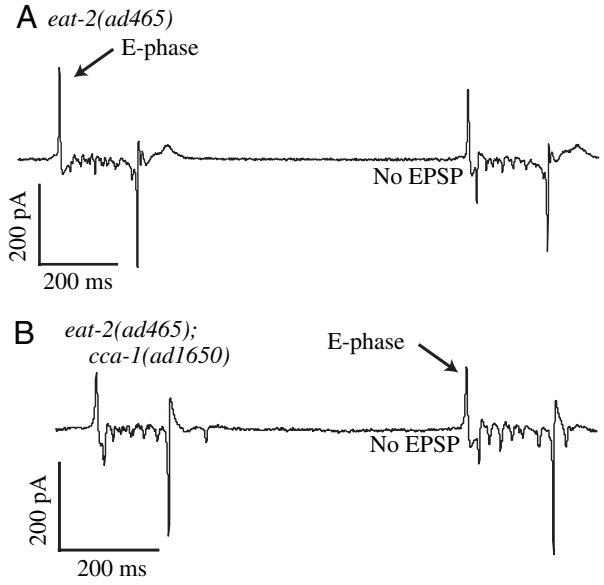

Fig. 6. Worms lacking the EAT-2 nicotinic receptor subunit initiate action potentials without MC-stimulated EPSPs. (A) EPGs from *eat-2* mutants lack EPSPs and I-phase spikes because *eat-2* mutants are defective in nicotinic neurotransmission from MC to the pharyngeal muscle. The *ad465* allele of *eat-2* contains an early stop codon. (B) EPGs from *eat-2; cca-1* double mutants closely resemble those of *eat-2* single mutants. E-phase spikes are marked with arrows.

in terms of viability and pumping rate (Fig. 3A). EPGs recorded from *eat-2; cca-1* double mutants lack EPSPs, and resemble EPGs recorded from *eat-2* single mutants (Fig. 6A,B). However, intracellular recordings reveal alterations in resting membrane potential that can explain the lack of interaction between *eat-2* and *cca-1* mutations: *eat-2* single mutants display a resting potential that is elevated by about 13 mV over wild-type resting potential (compare Fig. 7A and C, and see Fig. 7E; this is a statistically significant difference). More strikingly, resting potential in *eat-2* mutant pharynxes tends to be unstable and to spontaneously increase (Fig. 7D). Because this alteration in membrane potential cannot easily be explained as a direct result of the absence of the EAT-2 gene product, we suspect that it represents an adaptation employed by the pharynx to facilitate action potential generation. This adaptation may cause the membrane to spontaneously depolarize to a level at which the EGL-19 channel is activated, or may enhance the actions of some other current that brings the membrane to the EGL-19 threshold. In either case, the positive shift in membrane potential seems to allow the pharyngeal muscle to spontaneously depolarize without relying on calcium influx through CCA-1. Resting potential in *eat-2; cca-1* double mutants is elevated, but not significantly more than in *eat-2* single mutants (Fig. 7D,E). Yet, pumping is just as efficient in *eat-2; cca-1* double mutants as in *eat-2* single mutants (Fig. 3A). These results demonstrate that the pharynx adapts to the loss of nicotinic MC input by enhancing muscle excitability through changes in resting membrane potential. The process of adaptation allows the animal to preserve pharyngeal muscle activity and maintain feeding behavior, but makes the CCA-1 T-type channel less important.

Discussion

cca-1, which encodes the homolog of the T-type calcium channel family found in vertebrates, plays a crucial role in the initiation of action potentials in the pharyngeal muscle of *C. elegans.* The results described in this report have led us to propose a model of how CCA-1 acts with EAT-2, a non-alpha nicotinic receptor subunit, to initiate the activation of the EGL-19 L-type calcium channels present in pharyngeal muscle (Fig. 8). Cooperation between neurotransmitter receptors, T-type (LVA) channels and HVA calcium channels to achieve full depolarization of a cell has been proposed to occur in both pyramidal neurons and arterial smooth muscle, but has not been demonstrated at the genetic level (Gillessen and Alzheimer, 1997; Urban et al., 1998; Xi et al., 2002). CCA-1 channels appear to activate in response to the small membrane depolarizations (EPSPs) resulting from MC motor neuron stimulation of nicotinic receptors on the pharyngeal muscle surface. Calcium influx through CCA-1 channels may then lift membrane potential to the threshold for activation of EGL-19 L-type calcium channels. When CCA-1 is absent, the pharyngeal muscle action potential does not have a smooth, steep upstroke, but tends to dip or plateau early in depolarization. We believe the flattening of the upstroke results from the absence of calcium influx through CCA-1, which would normally begin at about –30 mV (Shtonda and Avery, 2005). Extracellular recordings also reveal that some MC EPSPs fail to trigger any muscle depolarization in *cca-1* mutants. Failure to respond to some EPSPs and slow depolarizations in response to others combine to significantly reduce the feeding rates of worms carrying mutations in *cca-1*.

Because CCA-1 activation appears to be the first step in the response of the pharyngeal muscle to MC stimulation, we predicted that CCA-1 activity would be critical in worms with defects in MC signaling. Mutations in *snt-1* (synaptotagmin) and *unc-17* (an acetylcholine vesicle transporter) reduce the amount of acetylcholine released when the MC neuron fires, and increase the frequency with which EPSPs fail to trigger full action potentials. Combining either of these mutations with a *cca-1* loss-of-function allele severely impairs pharyngeal pumping, and dramatically increases the failure rate of EPSPs. This result demonstrates that while CCA-1 activation seems to have only modest effects on action potential generation in wild-type worms, CCA-1 function becomes crucial when cholinergic transmission is reduced. Activity of T-type channels may therefore help to ensure that the pharyngeal muscle responds consistently and quickly to motor neuron stimulation, even in the face of reduced synaptic input. Zhang et al. (2004) have recently shown that T-type calcium currents are up-regulated in thalamic relay neurons when neurotransmitter release is compromised. Enhanced T-type

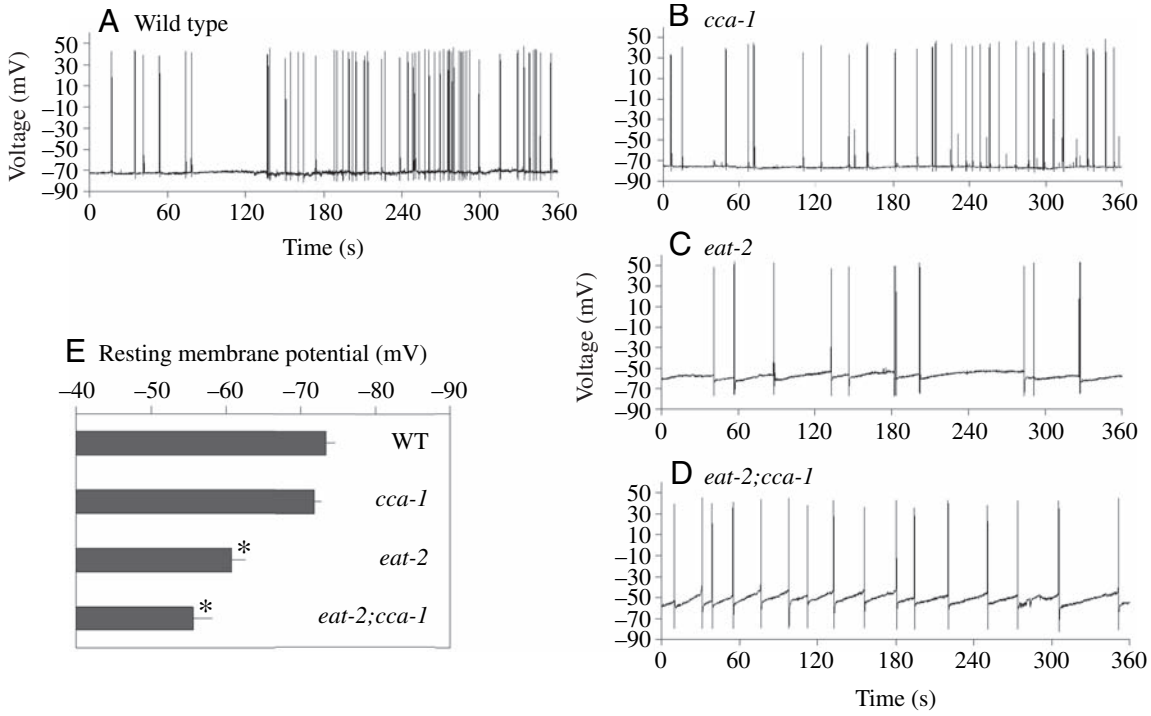

Fig. 7. Worms adapt to the loss of nicotinic MC stimulation by altering resting potential to preserve pharyngeal pumping. (A) Sample intracellular voltage recordings from wild-type worms show that resting potential is about –73 mV. (B) Resting potential in *cca-1* single mutants matches that of wild-type worms. (C) In contrast, a recording from an *eat-2* mutant reveals that resting potential is elevated by ~13 mV over wild-type resting potential, and has a slight tendency to rise between action potentials. (D) A recording from an *eat-2; cca-1* double mutant reveals an elevated resting potential that drifts significantly towards positive potentials between action potentials. (E) Average resting membrane potential for above four strains. Mean ± S.E.M.; *N*=12 (WT), 10 (*cca-1*), 15 (*eat-2*), 11 (*eat-2*; *cca-1*). *Significantly different from both the wild type and *cca-1* (P<0.005, *t*-test).

currents allow the affected thalamic neurons to maintain a high level of synaptic output to cortical neurons. T-type channels may therefore function in a variety of tissues to maintain effective levels of signaling in compromised circuits.

Unexpectedly, CCA-1 does not seem important when nicotinic signaling from MC is specifically abolished: adding a *cca-1* mutation to a strain lacking the EAT-2 nicotinic receptor subunit has little overt effect on pharyngeal pumping. Intracellular voltage recordings reveal that worms adapt to the loss of nicotinic MC input by altering the resting membrane potential of the pharyngeal muscle. Resting potential in both *eat-2* and *eat-2; cca-1* mutants is more positive than in wild-type worms, and tends to drift upwards in double mutant pharynxes. We speculate that this unstable membrane potential results from the activation of a leakage conductance that is normally obscured by frequent action potentials, but is upregulated in *eat-2; cca-1* double mutants to preserve pharyngeal muscle activity. Shtonda and Avery (2005) observed a weakly voltage-dependent, Ni^{2+}- and nifedipine-insensitive conductance that may be involved. Depolarization

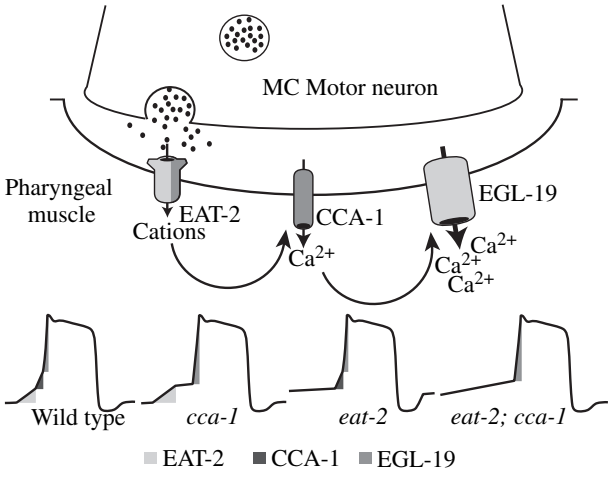

Fig. 8. Proposed role of the CCA-1 T-type channel in the pharyngeal action potential. In wild-type worms, action potentials are triggered by the influx of cations through the EAT-2-containing acetylcholine gated channel. The small rise in membrane potential resulting from cation influx is sufficient to activate the CCA-1 T-type channel. Calcium influx through CCA-1 lifts membrane potential further, until the EGL-19 L-type calcium channels can be activated. In the absence of CCA-1 function, some EPSPs fail to activate EGL-19 channels, or activate them more slowly than in wild-type worms. When both MC EPSPs and CCA-1 function are absent, the pharynx employs an alternative method, possibly a leak conductance and an elevation of resting membrane potential, to trigger EGL-19 activation.

by way of the leakage conductance may be able to bring the membrane to the threshold for EGL-19 activation, thus directly triggering an action potential, or may rely on additional intermediate steps that we have not yet identified. It is interesting that *snt-1; cca-1* and *unc-17; cca-1* double mutant worms do not successfully employ the same adaptive strategy used by *eat-2; cca-1* double mutants, and have severe feeding defects. This disparity suggests that adaptation requires a different form of cholinergic input (either from a source other than MC or through receptors other than nicotinic ones), and may explain why acetylcholine is essential for pumping (Avery and Horvitz, 1990) but EAT-2/EAT-18 pharyngeal nicotinic receptors are not. Additional characterization of the relationship of membrane potential to the activity of MC and other motor neurons will be required to clarify this issue.

The role we have described for CCA-1 channels in pharyngeal muscle depolarization is similar to the function described for T-type currents in the vertebrate heart. T-type currents in sino-atrial node and latent pacemaker cells mediate a late diastolic segment of depolarization, and serve as a bridge between the early pacemaker currents (I_f and I_k) and the opening of voltage gated sodium channels that mediate rapid depolarization (Hagiwara et al., 1988; Zhou and Lipsius, 1994). When T-type currents are blocked with nickel, the slope of the late diastolic depolarization is reduced, the fast upstroke is delayed and heart rate slows (Hagiwara et al., 1988; Satoh, 1995), in much the same way that pharyngeal pumping rate slows when *cca-1* is mutated. However, CCA-1 activates in response to neuronal input, rather than to muscle-intrinsic leak currents. It is therefore interesting to speculate that *C. elegans* may retain a leak current pacemaking mechanism, which becomes important when motor neuron input and CCA-1 activity are both compromised.

Because we have direct electrophysiological evidence of a CCA-1-mediated T-type current in the pharyngeal muscle, and because all the observed pharyngeal function defects in *cca-1* mutants can be explained by a role for CCA-1 in the muscle membrane, we have not discussed possible functions for CCA-1 outside the pharyngeal muscle. Perhaps the most likely site of an additional CCA-1 effect on feeding is the MC motor neuron, which expresses a *cca-1* reporter construct (Fig. S3 in supplementary material). Pan et al. (2001) reported that T-type channels contribute to neurotransmitter release in retinal bipolar cells, and the CCA-1 channel might play a similar role in MC. Disruption of acetylcholine release from MC might contribute to the inefficient feeding observed in *cca-1* mutants, and may explain some of the synergistic effects seen when *cca-1* mutations are combined with *snt-1* or *unc-17* mutations that reduce synaptic transmission. (As noted above, the maintenance of efficient pumping in the absence of nicotinic MC input may require other types of cholinergic signaling, which might be compromised in *cca-1* mutants.) However, effects within MC would not explain the alterations we have observed in voltage recordings from the pharyngeal muscle in *cca-1* mutants. Because we have not yet developed a rescuing *cca-1* construct, we cannot exclude a role for *cca-1* function in MC. Similarly, we cannot rule out the possibility that CCA-1 channels located outside the pharynx influence feeding behavior. We have observed no obvious defects in locomotion, egg-laying, defecation or mating in *cca-1* mutants (data not shown). However, loss of *cca-1* function may cause subtle defects in the activity of other excitable cells which are obscured by adaptive mechanisms such as that observed in *eat-2; cca-1* double mutants. The development of additional double mutant strains and careful electrophysiological analysis may therefore reveal roles for T-type conductances in other muscles and neurons.

In summary, this study has provided an initial characterization of the *cca-1* gene from *C. elegans*, and directly demonstrates a role for T-type currents in pharyngeal muscle depolarization. CCA-1 T-type channels participate in the initiation of action potentials, helping the membrane to reach the threshold for activation of L-type channels after an EPSP from the MC motor neuron. The importance of this function is suggested by both the impact on feeding behavior of loss of *cca-1* function, and the fact that the pharyngeal muscle undergoes considerable adaptive changes – altering membrane potential – in order to preserve muscle function in the absence of CCA-1 and motor neuron activity.

The *cca-1(gk30)* allele was provided by the *C. elegans* Reverse Genetics Core Facility at U.B.C., which is part of the International *C. elegans* Gene Knockout Consortium. We thank Kevin Hamming and Joseph Dent for comments on the manuscript. This research was supported by National Institutes of Health research grant HL46154 (to L.A.) and a grant from the Canadian Institutes for Health Research (CIHR, to T.P.S.). T.P.S. is the recipient of a CIHR Senior Investigator Award.

References

Albertson, D. G. and Thomson, J. N. (1976). The pharynx of *Caenorhabditis elegans*. *Phil. Trans. R. Soc. Lond. B* **275**, 299-325.

Alfonso, A., Grundahl, K., Duerr, J. S., Han, H. P. and Rand, J. B. (1993). The *Caenorhabditis elegans unc-17* gene: a putative vesicular acetylcholine transporter. *Science* **261**, 617-619.

Armstrong, C. M. and Matteson, D. R. (1985). Two distinct populations of calcium channels in a clonal line of pituitary cells. *Science.* **227**, 65-67.

Avery, L. (1993a). The genetics of feeding in *Caenorhabditis elegans. Genetics* **133**, 897-917.

Avery, L. (1993b). Motor neuron M3 controls pharyngeal muscle relaxation timing in *Caenorhabditis elegans*. *J. Exp. Zool.* **175**, 283-297.

Avery, L. and Horvitz, H. R. (1987). A cell that dies during wild-type *C. elegans* development can function as a neuron in a ced-3 mutant. *Cell* **51**, 1071-1078.

Avery, L. and Horvitz, H. R. (1989). Pharyngeal pumping continues after laser killing of the pharyngeal nervous system of *C. elegans*. *Neuron* **3**, 473-485.

Avery, L. and Horvitz, H. R. (1990). Effects of starvation and neuroactive drugs on feeding in *Caenorhabditis elegans*. *J. Exp. Zool.* **253**, 263-270.

Avery, L., Raizen, D. and Lockery, S. (1995). Electrophysiological methods. *Methods Cell Biol.* **48**, 251-269.

Bean, B. P. and McDonough, S. I. (1998). Two for T. *Neuron* **20**, 825-828.

Blumenthal, T. and Steward, K. (1997). RNA processing and gene structure. In *C. elegans II* (ed. D. Riddle, T. Blumenthal, B. Meyer and J. Priess), pp. 117-145. Cold Spring Harbor, NY: Cold Spring Harbor Laboratory Press.

Boyer, H. W. and Roulland-Dussoix, D. (1969). A complementation analysis

of the restriction and modification of DNA in *Escherichia coli*. *J. Mol. Biol.* **41**, 459-472.

Carbone, E. and Lux, H. D. (1984). A low voltage-activated, fully inactivating Ca channel in vertebrate sensory neurones. *Nature* **310**, 501-502.

Cohen, C. J., McCarthy, R. T., Barrett, P. Q. and Rasmussen, H. (1988). Ca channels in adrenal glomerulosa cells: K+ and angiotensin II increase T-type Ca channel current. *Proc. Natl. Acad. Sci. USA* **85**, 2412-2416.

Cribbs, L. L., Lee, J. H., Yang, J., Satin, J., Zhang, Y., Daud, A., Barclay, J., Williamson, M. P., Fox, M., Rees, M. et al. (1998). Cloning and characterization of alpha1H from human heart, a member of the T-type Ca2+ channel gene family. *Circ. Res.* **83**, 103-109.

Davis, M. W., Fleischhauer, R., Dent, J. A., Joho, R. H. and Avery, L. (1999). A mutation in the *C. elegans* EXP-2 potassium channel that alters feeding behavior. *Science* **286**, 2501-2504.

Dent, J. A., Davis, M. W. and Avery, L. (1997). *avr-15* encodes a chloride channel subunit that mediates inhibitory glutamatergic neurotransmission and ivermectin sensitivity in *Caenorhabditis elegans*. *EMBO J.* **16**, 5867-5879.

Doncaster, C. C. (1962). Nematode feeding mechanisms. I. Observations on *Rhabditis* and *Pelodera*. *Nematologica* **8**, 313-320.

Gillessen, T. and Alzheimer, C. (1997). Amplification of EPSPs by low Ni(2+)- and amiloride-sensitive Ca2+ channels in apical dendrites of rat CA1 pyramidal neurons. *J. Neurophysiol.* **77**, 1639-1643.

Hagiwara, N., Irisawa, H. and Kameyama, M. (1988). Contribution of two types of calcium currents to the pacemaker potentials of rabbit sino-atrial node cells. *J. Physiol.* **395**, 233-253.

Hansen, P. B., Jensen, B. L., Andreasen, D. and Skott, O. (2001). Differential expression of T- and L-type voltage-dependent calcium channels in renal resistance vessels. *Circ. Res.* **89**, 630-638.

Hobert, O. (2002). PCR fusion-based approach to create reporter gene constructs for expression analysis in transgenic *C. elegans*. *Biotechniques* **32**, 728-730.

Huguenard, J. R. (1996). Low-threshold calcium currents in central nervous system neurons. *Ann. Rev. Physiol.* **58**, 329-348.

Kim, D., Song, I., Keum, S., Lee, T., Jeong, M. J., Kim, S. S., McEnery, M. W. and Shin, H. S. (2001). Lack of the burst firing of thalamocortical relay neurons and resistance to absence seizures in mice lacking alpha(1G) T-type Ca(2+) channels. *Neuron* **31**, 35-45.

Lee, J. H., Daud, A. N., Cribbs, L. L., Lacerda, A. E., Pereverzev, A., Klockner, U., Schneider, T. and Perez-Reyes, E. (1999). Cloning and expression of a novel member of the low voltage-activated T-type calcium channel family. *J. Neurosci.* **19**, 1912-1921.

Lee, R. Y., Lobel, L., Hengartner, M., Horvitz, H. R. and Avery, L. (1997). Mutations in the alpha1 subunit of an L-type voltage-activated Ca^{2+} channel cause myotonia in *Caenorhabditis elegans*. *EMBO J.* **16**, 6066-6076.

Maupas, E. (1900). Modes et formes de reproduction dés nematodes. *Arch. Zool. Exp. Genet.* **8**, 463-624.

McKay, J., Raizen, D., Gottschalk, A., Schafer, W. and Avery, L. (2003). eat-2 and eat-18 are required for nicotinic neurotransmission in the *C. elegans* pharynx. *Genetics* **166**, 161-169.

McRory, J. E., Santi, C. M., Hamming, K. S., Mezeyova, J., Sutton, K. G., Baillie, D. L., Stea, A. and Snutch, T. P. (2001). Molecular and functional characterization of a family of rat brain T-type calcium channels. *J. Biol. Chem.* **276**, 3999-4011.

Monteil, A., Chemin, J., Bourinet, E., Mennessier, G., Lory, P. and Nargeot, J. (2000a). Molecular and functional properties of the human alpha(1G) subunit that forms T-type calcium channels. *J. Biol. Chem.* **275**, 6090-6100.

Monteil, A., Chemin, J., Leuranguer, V., Altier, C., Mennessier, G., Bourinet, E., Lory, P. and Nargeot, J. (2000b). Specific properties of T-type calcium channels generated by the human alpha 1I subunit. *J. Biol. Chem.* **275**, 16530-16535.

Nilius, B., Hess, P., Lansman, J. B. and Tsien, R. W. (1985). A novel type of cardiac calcium channel in ventricular cells. *Nature* **316**, 443-446.

Nonet, M. L., Grundahl, K., Meyer, B. J. and Rand, J. B. (1993). Synaptic function is impaired but not eliminated in *C. elegans* mutants lacking synaptotagmin. *Cell* **73**, 1291-1305.

Pan, Z. H., Hu, H. J., Perring, P. and Andrade, R. (2001). T-type Ca(2+) channels mediate neurotransmitter release in retinal bipolar cells. *Neuron* **32**, 89-98.

Perez-Reyes, E. (2003). Molecular physiology of low-voltage-activated t-type calcium channels. *Physiol. Rev.* **83**, 117-161.

Perez-Reyes, E., Cribbs, L. L., Daud, A., Lacerda, A. E., Barclay, J., Williamson, M. P., Fox, M., Rees, M. and Lee, J. H. (1998). Molecular characterization of a neuronal low-voltage-activated T-type calcium channel. *Nature* **391**, 896-900.

Raizen, D. M. and Avery, L. (1994). Electrical activity and behavior in the pharynx of *Caenorhabditis elegans*. *Neuron* **12**, 483-495.

Raizen, D. M., Lee, R. Y. and Avery, L. (1995). Interacting genes required for pharyngeal excitation by motor neuron MC in *Caenorhabditis elegans*. *Genetics* **141**, 1365-1382.

Regan, M. R., Emerick, M. C. and Agnew, W. S. (2000). Full-length single-gene cDNA libraries: Applications in splice variant analysis. *Anal. Biochem.* **286**, 265-276.

Satoh, H. (1995). Role of T-type Ca^{2+} channel inhibitors in the pacemaker depolarization in rabbit sino-atrial nodal cells. *Gen. Pharmacol.* **26**, 581-587.

Seymour, M. K., Wright, K. A. and Doncaster, C. C. (1983). The action of the anterior feeding apparatus of *Caenorhabditis elegans* (Nematoda: Rhabditida). *J. Zool.* **201**, 527-539.

Shtonda, B. B. and Avery, L. (2005). CCA-1, EGL-19 and EXP-2 currents shape action potentials in the *Caenorhabditis elegans* pharynx. *J. Exp. Biol.* **208**, 2177-2190.

Sulston, J. E. and Hodgkin, J. (1988). Methods. In *The Nematode* C. elegans (ed. W. Wood), pp. 587-606. Cold Spring Harbor, New York: Cold Spring Harbor Laboratory.

Urban, N. N., Henze, D. A. and Barrionuevo, G. (1998). Amplification of perforant-path EPSPs in CA3 pyramidal cells by LVA calcium and sodium channels. *J. Neurophysiol.* **80**, 1558-1561.

Xi, Q., Ziogas, J., Roberts, J. A., Evans, R. J. and Angus, J. A. (2002). Involvement of T-type calcium channels in excitatory junction potentials in rat resistance mesenteric arteries. *Br. J. Pharmacol.* **137**, 805-812.

Zhang, Y., Vilaythong, A. P., Yoshor, D. and Noebels, J. L. (2004). Elevated thalamic low-voltage-activated currents precede the onset of absence epilepsy in the SNAP25-deficient mouse mutant coloboma. *J. Neurosci.* **24**, 5239-5248.

Zhou, Z. and Lipsius, S. L. (1994). T-type calcium current in latent pacemaker cells isolated from cat right atrium. *J. Mol. Cel. Cardiol.* **26**, 1211-1219.